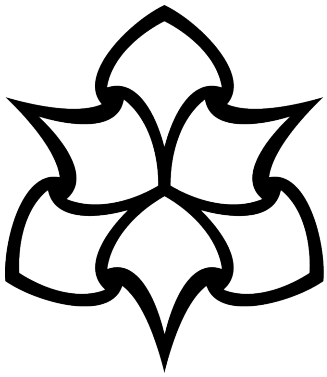

Manchester Metropolitan University

Jahan, N and Rahman, MD M and Ahsan, Mominul and Based, Md Abdul and Rana, MM and Gurusamy, Saravanakumar and Haider, Julfikar (2021) Photonic Crystal Fiber Based Biosensor for Pseudomonas Bacteria Detection: A Simulation Study. IEEE Access, 9. pp. 42206-42215. ISSN 2169-3536

Downloaded from: http://e-space.mmu.ac.uk/627353/

Version: Published Version

Publisher: Institute of Electrical and Electronics Engineers (IEEE)

DOI: https://doi.org/10.1109/ACCESS.2021.3063691

Usage rights: Creative Commons: Attribution 4.0

Please cite the published version

https://e-space.mmu.ac.uk

IEEE Access
Multidisciplinary | Rapid Review | Open Access Journal

Received February 6, 2021, accepted February 26, 2021, date of publication March 4, 2021, date of current version March 22, 2021.

Digital Object Identifier 10.1109/ACCESS.2021.3063691

Photonic Crystal Fiber Based Biosensor for Pseudomonas Bacteria Detection: A Simulation Study

N. JAHAN[1], MD. M. RAHMAN[1], MOMINUL AHSAN[2], MD. ABDUL BASED[3], (Member, IEEE), MD. MASUD RANA[4], SARAVANAKUMAR GURUSAMY[5], (Member, IEEE), AND JULFIKAR HAIDER[2]

[1]Department of Electrical and Computer Engineering, Rajshahi University of Engineering and Technology, Rajshahi 6204, Bangladesh
[2]Department of Engineering, Manchester Metropolitan University, Manchester M1 5GD, U.K.
[3]Department of Electrical, Electronics and Telecommunication Engineering, Dhaka International University, Dhaka 1205, Bangladesh
[4]Department of Electrical and Electronic Engineering, Rajshahi University of Engineering and Technology, Rajshahi 6204, Bangladesh
[5]Department of Electrical and Electronics Technology, Federal Technical and Vocational Education and Training (TVET) Institute, Addis Ababa 190310, Ethiopia

Corresponding author: Saravanakumar Gurusamy (saravanakuma.gurusamy@ftveti.edu.et)

ABSTRACT The detection of microorganisms like *Pseudomonas* are very important as they trigger an infection in human blood, lungs, and different parts of the body causing various ailments. In this paper, a surface plasmon resonance (SPR) biosensor based on photonic crystal fiber (PCF) has been proposed to detect the presence of *Pseudomonas* bacteria with attractive performance characteristics. The sensor is designed using a simple circular lattice of PCF, coated with a thin chemically stable gold layer. The performance investigation of the sensor is numerically carried out by using a finite element (FE) based simulation tool where the highest wavelength and amplitude sensitivity are found as 20,000 nm/RIU and 1380 RIU^{-1}, respectively. The sensor shows an excellent spectral resolution of the highest value of 5.26×10^{-6} RIU, ensuring the capability of identifying a very small change in analyte refractive index (RI) within the range of 1.33 to 1.42. The performance investigation is also carried out altering the diameter of air holes, pitch, and gold layer thickness to explore the variation in phase matching conditions due to the change in structural parameters. As the sensor is adept at detecting the sample with high sensitivity and sensing resolution, the proposed sensor can be highly efficient in detecting *Pseudomonas* bacteria as well as other organic compounds, and biological analytes.

INDEX TERMS Biosensor, *Pseudomonas* bacteria, sensitivity, FEA, SPR.

I. INTRODUCTION

Pseudomonas, a genus of bacteria belonging to the *Pseudomonadaceae* family, is regularly found in nature, such as soil, water, plants, animals, and humans. It was first identified in 1882 by Gessard [1]. *Pseudomonas* is a pervasive opportunistic pathogen that triggers human infections called *Pseudomonas aeruginosa*, resulting in diseases in blood, lungs (pneumonia), or different parts of the body after a medical procedure. This bacteria spreads through the debased water, soil, and nourishment. *Pseudomonas aeruginosa* infections are commonly settled with antitoxins, however, the bacteria find new ways for keeping away from the impact of anti-infection agents. The casualty rate due to *Pseudomonas aeruginosa* is high as a direct result of the resistant reaction, debilitated anti-microbial, and the bacterial exoenzymes that have been produced [2]. To apply the best anti-infection agents for settling such infections, the blood samples are sent to a research laboratory to culture and test the bacteria developed against a lot of antitoxins and figure out which are the dynamics against the microbes [3].

Nowadays, surface plasmon resonance (SPR) based sensors are widely used in environmental monitoring, disease detection, chemical sensing, and so on [4]–[8]. The main perception of SPR has found through a hypothetical path by *Ritchie et al.* during the 1950s [9]. SPR occurs at the interface of two opposite permittivity materials due to stimulated oscillation of the conduction electrons by a transverse magnetically (TM) -polarized light. The oscillating free electrons consume this photon energy which causes the generation

The associate editor coordinating the review of this manuscript and approving it for publication was Sanket Goel.

This work is licensed under a Creative Commons Attribution 4.0 License. For more information, see https://creativecommons.org/licenses/by/4.0/

and proliferation of surface plasmon wave (SPW) at the interface [10]. So far, various SPR sensors utilizing different light coupling technology have been reported. Among them, prism [11]–[13], conventional optical fiber (OF) [14], [15] photonic crystal fiber (PCF) [16], [17] based SPR sensors are widely studied. The performance of SPR sensors is strongly dependent on the plasmonic materials and in most cases, gold (Au) and silver (Ag) are commonly used. Yet Au is preferred since it is impervious to oxidation and erosion under various environments [13]. In addition, Au shows a larger wavelength shift that facilitates the ease of detection of an unknown analyte precisely [18]. Although silver's resonance peak is very sharp and it shows higher detection precision contrasted with gold, it gets oxidized frequently [19]. Therefore, owing to higher chemical stability and superior performance, gold is often used as plasmonic material [20].

To date, numerous works have been done to detect the *Pseudomonas* bacteria using different technologies [21]–[23], but SPR based sensor has gained much more attention owing to its versatile properties and level-free real-time detection capability [3], [24]. Verma *et al.* [24] introduced an SPR sensor using the graphene-based configuration for the detection of *Pseudomonas*-like bacteria. Another research group has recently proposed an SPR sensor [25], with improved sensitivity using graphene and chalcogenide. Likely, Kushwaha *et al.* [3] developed an SPR sensor for a similar purpose using Zinc oxide, gold, and graphene. More recently, Mudgal *et al.* [2] proposed an SPR sensor using silver, barium titanate, graphene, and affinity coat to identify the *Pseudomonas* bacteria. All the above researchers proposed SPR sensors using prism coupler operating on the angular interrogation method. Nevertheless, the prism-based sensors are massive and are limited to remote sensing applications. On the other hand, conventional optical fiber (OF) based sensors are limited to their design parameters [20]. By using PCF rather than the prism and the conventional OF, these limitations can be overcome [26], [27].

In this paper, a PCF based SPR sensor is proposed for the detection of microorganisms like *Pseudomonas* using wavelength interrogation (WI) as well as amplitude interrogation (AI) approach to overcome the limitations of the prism-based sensor. The characterization of the proposed sensor is assessed in this work by varying the sensing medium RI from 1.33 to 1.42. While designing a simple geometrical structure with an external sensing scheme is considered for ease of fabrication and operation. In addition to higher sensitivity, the proposed sensor shows an admirable amplitude sensing response that is explored using the finite element method (FEM) based software. In addition, the fabrication tolerance due to variation of air hole diameters, pitch, the thickness of plasmonic material, etc. is extensively investigated for evaluating optimal performance of the proposed sensor.

II. MODELLING OF THE SENSOR

The researchers have attempted to develop different compositions and configurations over the last few decades to achieve better performance of PCF based sensors by featuring new methods and concepts. Fig. 1. (a) exhibits the 2-D view of the proposed SPR sensor, where a single air hole ring is considered for designing the sensor. The center–to–center distance of two contiguous air holes, known as the pitch is considered to be $p = 1.5\ \mu m$ where all the air holes within the ring are spaced at 30° apart. In this ring, two different air holes are used where the larger air holes consist of the diameter of $D = 0.2 \times p\ \mu m$. The smaller air hole positioned at 60°, 120°, 240°, and 300° are of the diameter of $D_1 = 0.75 \times D\ \mu m$ that helps to create a channel to drive more light through the metal interface resulting in a more evanescent field. The innermost air hole with a diameter of D_1 forms a hollow core structure. Also, two similar air holes that help in phase matching of the sensor are placed just rightward and leftward direction of the centered one [5]. The thickness of the gold layer coating

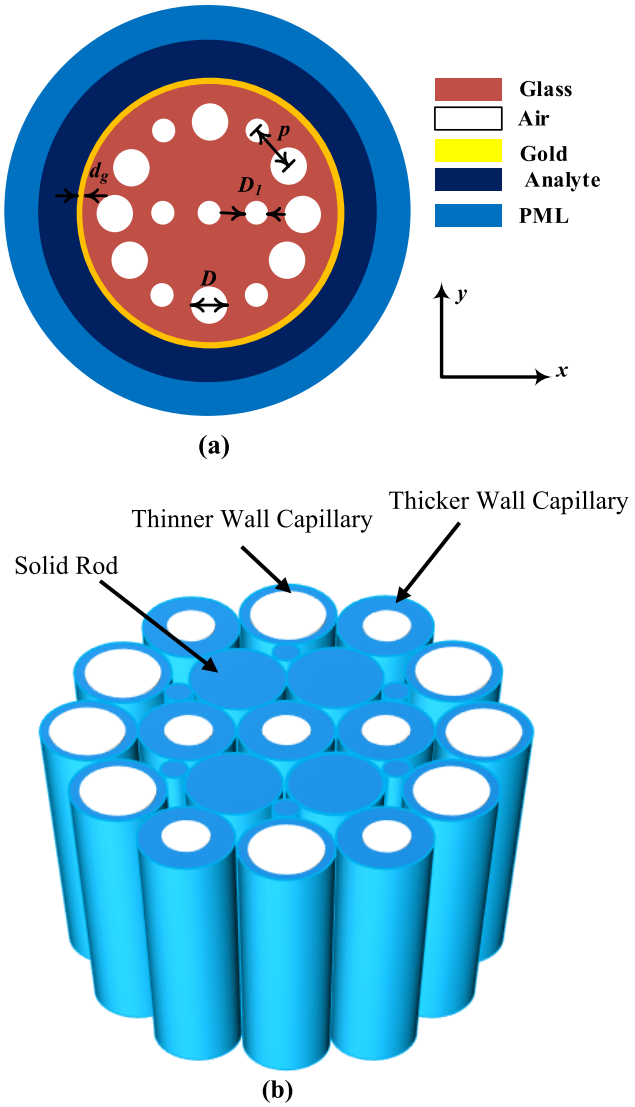

FIGURE 1. (a) 2–D view of the proposed PCF based SPR sensor and (b) stacked preform assembly for PCF formulation.

upon the PCF is considered to be $d_g = 30\ nm$. Fused silica is utilized as the foundation material to manufacture the PCF structure and the Sellmeier equation is used for determining the RI of the silica [28]. Furthermore, the dielectric constant of Au is calculated using the Drude–Lorenz model [29].

For evaluating the sensing performance, confinement loss plays a significant preface which is obtained by the accompanying equation [30],

$$\alpha = 8.686 \times k_0 \times \mathrm{Im}[n_{eff}] \times 10^4 \tag{1}$$

Here α is the confinement loss in dB/cm where k_0 indicates the free space wave vector that equal to $2\pi/\lambda$. Also, $\mathrm{Im}[n_{eff}]$ indicates the imaginary part of the effective RI. To estimate the performance of the PCF based sensor, both the WI and AI approach can be applied. The wavelength sensitivity (WS) applying the WI method can be determined by the accompanying equation as follows [7]:

$$S_\lambda = \frac{\Delta\lambda_{peak}}{\Delta n_a} \tag{2}$$

Here S_λ indicates the WS in nm/RIU where $\Delta\lambda_{peak}$ and Δn_a are the difference of wavelength peak shifts and analyte RI variation, respectively. A sensor's ability to identify the slightest change in analyte RI can be estimated by using another performance measuring parameter called sensor resolution that can be calculated utilizing the accompanying equation as follows [31]:

$$R_\lambda = \frac{\Delta n_a \times \Delta\lambda_{\min}}{\Delta\lambda_{peak}} \tag{3}$$

Here, R_λ indicates the sensor resolution in RIU where $\Delta\lambda_{min}$ is the minimum spectral resolution of the sensor, and the value is supposed as $\Delta\lambda_{\min} = 0.1$ nm [31], [32].

The estimation of the WS and its implementation is an expensive and sophisticated process as this method requires the complete spectra investigation of the signal [31]. Going with the AI approach is cost-effective because it estimates sensitivity at a consistent wavelength. The amplitude sensitivity (AS) of the sensor can be assessed utilizing the accompanying equation [33]:

$$S_A = -\frac{1}{\alpha(\lambda, n_a)} \frac{\Delta\alpha(\lambda, n_a)}{\Delta n_a} \tag{4}$$

Here, S_A indicates the AS in RIU^{-1}. Also, $\alpha(\lambda, n_a)$ and $\Delta\alpha(\lambda, n_a)$ denote the propagation loss for a selected analyte RI and the difference between two adjacent loss spectra, separately. Some essential parameters also describe the quality of a sensor, e.g., the figure of merit (FOM), signal–to–noise ratio (SNR), and detection limit (ϕ_n) which are directly allied to the full width at half maxima ($\Delta\lambda_{1/2}$) of the loss spectra and can be calculated with the following equations [34]:

$$FOM = \frac{S_\lambda}{\Delta\lambda_{1/2}} \tag{5}$$

$$SNR = \frac{\Delta\lambda_{peak}}{\Delta\lambda_{1/2}} \tag{6}$$

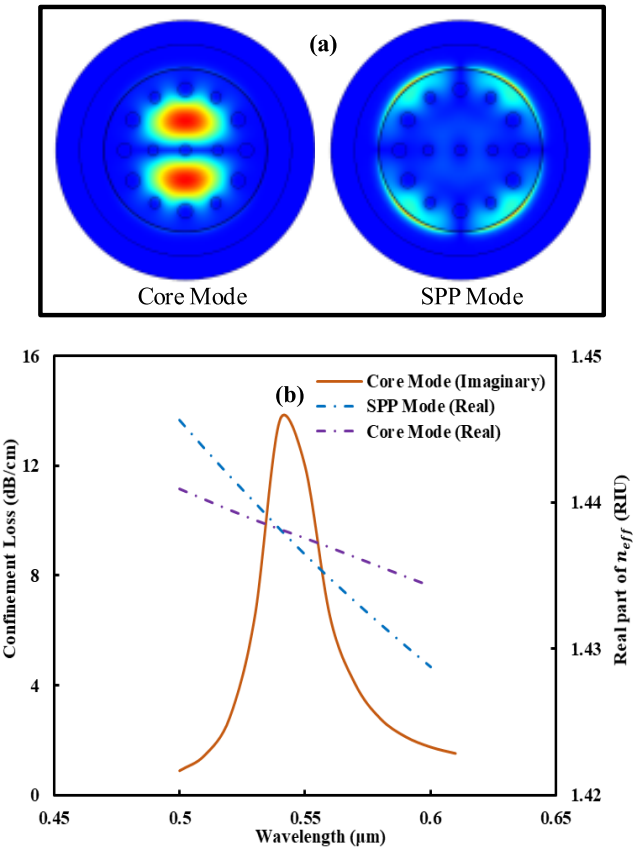

FIGURE 2. (a) Optical field scattering of the proposed sensor indicating the core guided mode and SPP mode for y–polarized light, (b) dispersion relation for y–polarized light indicating the phase matching condition of core mode and SPP mode for analyte RI of 1.33.

$$\phi_n = \frac{\Delta\lambda_{1/2}}{1.5 \times (SNR)^{0.25}} \tag{7}$$

The confinement factor is very important for the high index contrast waveguide to evaluate the modal gain. In the case of a low index contrast scheme, the electric and magnetic field distributions can be related by only a proportionality constant while the high index contrast system differs it [35], [36]. In this proposed sensor, due to low the index contrast the confinement factor can slightly affect the performance, and therefore it is avoided intentionally. As regards the fabrication of the proposed sensor, the PCF could be produced at first. Due to a simple circular geometrical structure, the proposed PCF could easily be fabricated applying the standard stack and draw method [37]. Fig. 1. (b) shows the preform structure that could be drawn in a standard drawing tower to realize the PCF. The smaller and bigger air holes are built by using the thicker and thin wall capillaries and the omitted air holes are replaced by solid glass rods to form the complete structure. A thin gold coating could be added after PCF fabrication to finalize the sensor structure. This process could be performed by using the chemical vapor deposition (CVD) technique [38]. Recently, another deposition technique called the atomic layer deposition (ALD) method has been introduced

TABLE 1. The simulation parameter for extra fine meshing in comsol multiphysics software.

Total computational area	92.54 μm^2
No. of triangular elements	17092
Vertex elements	76
Edge elements	1332
Total PML area	31 μm^2
No. of triangular elements of PML	200

to deposit an identical gold coating on the fiber exterior area [39].

III. NUMERICAL RESULTS ANALYSIS

The penetration of the evanescent field through the PCF and metal is vital to produce the surface plasmon wave. As the evanescent field hits the metal surface then the loosely bound electrons are excited triggering the generation of SPW. In the case of PCF based sensor maximum energy is transferred to the exciting electrons at resonance condition. At this condition, a significant amount of photon energy is absorbed by the free electrons causing a sharp loss peak. Fig. 2. (a) and (b) show the optical field scattering and dispersion characteristics of the proposed sensor for analyte RI of 1.33. The confinement loss is indicated by the solid line in Fig. 2 (b). The dotted violet and blue line indicate the phase matching of core mode and SPP mode, at the wavelength of 0.54 μm where both the line intersect one another. Provided that the proposed model is non–uniform, there will be a difference between the electric field near the metal surface for x– and y–polarized light. Both x– and y–polarized modes of light are considered for analysis to better characterize the proposed sensor. The modeling and simulation of the proposed sensor are performed using the FEM based COMSOL multiphysics software. Physics–controlled mode with extra fine meshing element size is used to get higher simulation precision. The simulation parameters are listed in Table 1. In modeling of the sensor, a perfectly matched layer (PML) is used as an ideal radiation absorber.

The variety of sensing medium RI significantly influences the SPR sensor's performances. Fig. 3 shows the confinement loss and AS of the proposed sensor subjected to specific analyte RI on the wavelength of the incident light. It is observed from Fig. 3. (a) that the peak losses (in dB/cm) are 40, 50, 60, 75, 100, 156, 280, 460, 466, and 560 for $x-$polarization of light for analyte RI of 1.33 to 1.42 with an interval of 0.01. On the other hand, from Fig. 3. (b) the peak losses (in dB/cm) are observed as 10, 15, 20, 25, 35, 55, 90, 190, 480, and 475 for y–polarized light for the similar variation of analyte RI. It can be noticed that the loss curve's peak point deepens and shifts to overlong wavelength steadily while differing the analyte RI from 1.33 to 1.42.

It may be pragmatic from Fig. 3. (a)–(b) that for $x-$polarized light the SPR point shifts 20 nm, 30 nm, 40 nm, 40 nm, 50 nm, 70 nm, 90 nm, 160 nm, and 190 nm, respectively, for sensing medium RI variation of 1.33–1.34, 1.34–1.35, 1.35–1.36, 1.36–1.37, 1.37–1.38, 1.38–1.39, 1.39–1.40, 1.40–1.41, 1.41–1.42. Also, for y–polarized light, it shifts to 20 nm, 30 nm, 30 nm, 40 nm, 50 nm, 70 nm, 90 nm, 165 nm, and 200 nm for similar alteration. Utilizing equation (2) the WS (in nmRIU^{-1}) of the proposed sensor is found as 2000, 3000, 4000, 4000, 5000, 7000, 16000, and 19000 for x–polarized light for analyte RI of 1.33 to 1.42 with an interval of 0.01 as shown in Table 2. For y–polarized light, the sensor offers the WS (in nmRIU^{-1}) of 2000, 3000, 3000, 4000, 5000, 7000, 9000, 16500, and 20000 for a similar change of analyte RI. The maximum WS of the sensor is noted as 19000 nmRIU^{-1} and 20000 nmRIU^{-1} for x– and y–polarization of light, respectively. As well, the spectral resolution of the sensor is calculated by using equation (3) where the maximum and minimum value is found as 5×10^{-5} RIU and 5×10^{-6} RIU for x–polarization of light, and 4×10^{-5} RIU and 5.26×10^{-6} RIU for y–polarization of light.

Another performance indicating factor of the sensor is the AS that is calculated by applying equation (4) as depicted in Fig. 3. (c)–(d) for both the $x-$ and $y-$polarized light for analyte RI of 1.33 to 1.41. From Fig. 3. (c), it's observed that for x–polarized light the proposed sensor shows the AS (in RIU^{-1}) of 400, 440, 520, 600, 780, 1040, 1160, 500, and 240 for analyte RI of 1.33, 1.34, 1.35, 1.36, 1.37, 1.38, 1.39, 1.40, and 1.41, respectively. Also, for y–polarized light the AS (in RIU^{-1}) is found as 390, 420, 490, 580, 700, 890, 1190, 1380, and 540 for the same analyte RIs as depicted in Fig. 3. (d). The highest value of the AS for x–polarized light is observed as 1160 RIU^{-1} with $n_a = 1.39$ and for y–polarized light it is calculated as 1380 RIU^{-1} with $n_a = 1.40$. From the analysis, it can be expected that y–polarized mode offers better performance than x–polarized, and hence the further analysis (e.g. influence of variation of gold layer thickness, pitch, diameter, etc. on the sensor performance) is performed for y–polarized mode only. It can be also found from Fig. 3 that the sensor can be operated at light wavelengths from 0.5 microns to 1.3 microns.

The confinement loss of PCF-based sensor that is very relevant to the sensor length or propagation length depends on the fundamental structural parameters e.g., air hole rings in the cladding, the size of the air holes, the pitch of the air hole rings of the sensor [40], [41]. Besides, the core size and the operating wavelength of light are also important design parameters related to the confinement loss [41], [42]. In this proposed design, a relatively higher core length is considered. Furthermore, the distance between the air hole to air hole is kept small to facilitate lower leakage of light from the core to the cladding area, resulting in lower confinement loss. On the other hand, the sensor length or propagation length which depends on the confinement loss is also an important parameter. Some of the researchers reported that the millimeter range fiber could be used to detect the analyte RI [43]. The propagation length or sensor length (S_l) of a sensor and the confinement loss (α) are related by Equation 8 [44], [45]. Table 3 compares the confinement loss and sensor length of

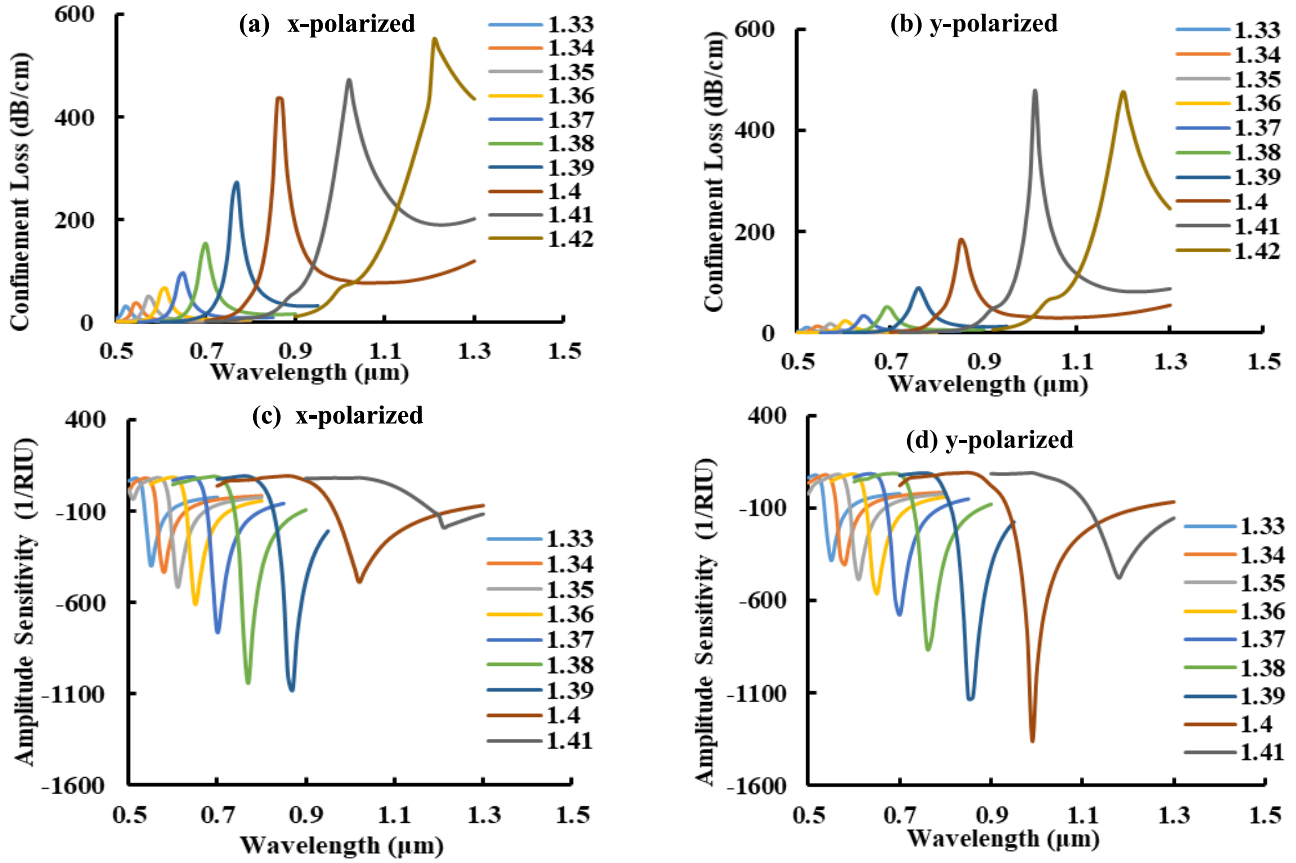

FIGURE 3. Variation in (a)–(b) confinement loss, and (c)–(d) amplitude sensitivity of the sensor due to alteration in sensing medium RI from 1.33 to 1.42 for x-and y-polarization of light, respectively.

TABLE 2. The performance characteristics of the proposed SPR sensor for Y–polarized Mode.

Analyte RI	SPR point (nm)	AS (RIU^{-1})	WS (nm/ RIU)	FWHM (nm)	SNR	FOM ($RIU^{-1)}$	DL (nm)
1.33	520	-382.92	2000	23.5	1.44	85.1	16.31
1.34	540	-405.08	3000	28.5	1.52	105.3	18.76
1.35	570	-485.51	3000	30.5	1.49	98.4	20.42
1.36	600	-562.31	4000	35.0	1.55	114.3	22.57
1.37	640	-677.01	5000	39.5	1.59	126.6	24.83
1.38	690	-858.45	7000	45.0	1.68	155.6	26.86
1.39	760	-1128.8	8500	46.5	1.74	182.8	26.66
1.40	850	-1360.1	16500	50.0	2.02	330.0	24.73
1.41	1010	-477.47	20000	42.5	2.21	470.	19.24
1.42	1200	–	–	150	–	–	–

some prior reported sensors [46], [10] with the proposed one.

$$S_l = \frac{1}{\alpha} \tag{8}$$

The value of full width at half maxima (FWHM) should be smaller to get higher sensor FOM and SNR to achieve better performance. Observing Fig. 3 (a)–(b), it is apparent that the FWHM gets increasing while rising the RI of the sensing medium. The FOM, SNR, and detection limit of the proposed sensor are determined using equations 5, 6, and, 7, respectively, which are tabulated in Table 2. It is noted that the FOM and SNR's highest value is found as 470.59 RIU^{-1} and 2.209, respectively. The resonance wavelength of the sensor is plotted for y–polarized light in Fig. 4 and the regression equation of the resonance wavelength as a function of analyte RI is determined using polynomial fitting which helps in the interpolation of the SPR point of the sensor in this region. The regression equation is found as $\lambda_{res} = 92424n_a^2 - 247488n_a + 166214$ with $R^2 = 0.9891$; where λ_{res} and n_a indicate the resonance wavelength and analyte RI, respectively. Finally, practical applications, detection technique, and coupling mechanism of some prior reported SPR based sensors and the proposed one are presented in Table 4.

IV. IMPACT DUE TO ALTERATION OF STRUCTURAL PARAMETERS ON SENSOR CHARACTERISTICS

The plasmonic material gold significantly impacts the performance of the proposed sensor. Fig. 5 exhibits the loss and AS curves of the sensor varying gold layer thickness of 30 nm to 45 nm for analyte RI of 1.37 and 1.38 where other parameters

TABLE 3. Table of comparison indicating the confinement loss and sensor length among the proposed sensor with some previously reported sensors.

Analyte RI	Reported sensor [46] by Lou et al.				Reported sensor [47] by Rifat et al.		Proposed sensor	
	Confinement loss with graphene layer (dB/cm)	Sensor Length (mm)	Confinement loss without graphene layer (dB/cm)	Sensor Length (mm)	Confinement loss layer (dB/cm)	Sensor Length (mm)	Confinement loss (dB/cm)	Sensor Length (mm)
1.33	172.84	0.0579	283.65	0.0353	138	0.0725	10	1.00
1.34	169.28	0.0059	278.80	0.0359	125	0.0800	15	0.6667
1.35	165.58	0.0061	275.44	0.0363	118	0.0847	20	0.5000
1.36	162.97	0.0061	273.80	0.0365	105	0.0952	25	0.4000
1.37	163.68	0.0061	279.59	0.0358	85	0.1176	35	0.2857
1.38	184.53	0.0054	322.66	0.0310	Not calculated	-	55	0.1818
1.39	Not calculated	-	Not calculated	-	Not calculated	-	90	0.1111
1.40	Not calculated	-	Not calculated	-	Not calculated	-	190	0.0526
1.41	Not calculated	-	Not calculated	-	Not calculated	-	480	0.0208
1.42	Not calculated	-	Not calculated	-	Not calculated	-	475	0.0211

TABLE 4. Application, detection technique, and coupling mechanism of some prior reported SPR sensors and the proposed one.

Ref.	Application of the sensor	Coupling device	Interrogation Technique
[2]	Pseudomonas Bacteria detection	Prism	Angle
[3]	Pseudomonas bacteria detection	Prism	Angle
[48]	Cancer cell detection	Optical Fiber	Wavelength
[49]	Glucose detection	Optical Fiber	Wavelength
[50]	Antibody detection	Optical Fiber	Wavelength
[51]	Breast cancer detection	Prism	Angle
[52]	Antibody detection	Optical Fiber	Wavelength
Proposed Work	Pseudomonas bacteria detection	Optical Fiber	Wavelength
Proposed Work	Pseudomonas bacteria detection	Optical Fiber	Amplitude

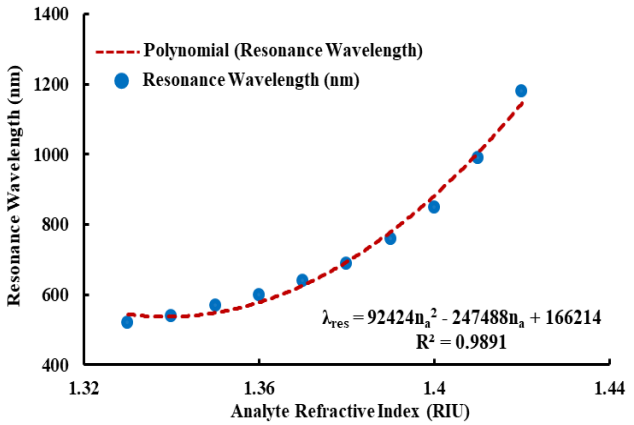

FIGURE 4. The regression analysis of the proposed sensor for y-polarized light using polynomial curve fitting of the resonance wavelength of the loss curves in terms of analyte RI.

remain unaltered. It's observed from Fig.5. (a) that the peak of the loss curves drops as a result of the rise in gold layer width. With the expansion of the gold layer width from 30 nm to 35 nm, 40 nm, and 45 nm, the reduced amount of peak losses (in dB/cm) are found as 6, 5, 16 and 6, 10, 23 for analyte RI of 1.37 and 1.38, respectively. It is also observed that, with the extension of the gold layer width, the peak loss is shifted to an overlong wavelength with an indication of descending inclination. The resonance peak for a thicker gold layer declines as a result of the damping attributes of the gold. Conversely, the narrow gold layer expands the deepness of loss curves. In this manner for light entrance, a thicker gold layer requires a longer wavelength. Henceforth, the peak loss is shifted with an expanding gold layer thickness. In addition, Fig. 5. (b) shows the impact of the gold layer on the AS of the sensor. It is observed from Fig. 5 that the sensor affords the highest AS and spectral loss for the gold layer width of 30 nm. The thickness of plasmonic material is considered as 30 nm for further analysis.

The distance between the metallic layer and sensor core as well as the distance between the air holes significantly affect the performance of the sensor. Although higher accuracy is maintained, it can happen that the designed parameters e.g., air holes diameter and pitch can be changed slightly during the fabrication process. In this analysis, the characterization of the sensor is performed by varying the pitch and diameter of air holes up to $\pm$ 5% of the designed parameter. Pitch is one of the considerable parameters for designing a PCF based SPR sensor. Confinement and propagation of light through the fiber requires an appropriate distance between the air holes. The effect of variation of pitch on the confinement loss and AS is depicted in Fig. 6. The curves indicated by the solid and dotted line in Fig. 6(a) displays the confinement loss for analyte RI of 1.37 and 1.38, separately. It can be found that the peak loss rises gradually and shifts towards the shorter wavelength with the increment of the pitch as the structure allow more energy to transfer from the center to the cladding region. As well, the sensor shows the opposite

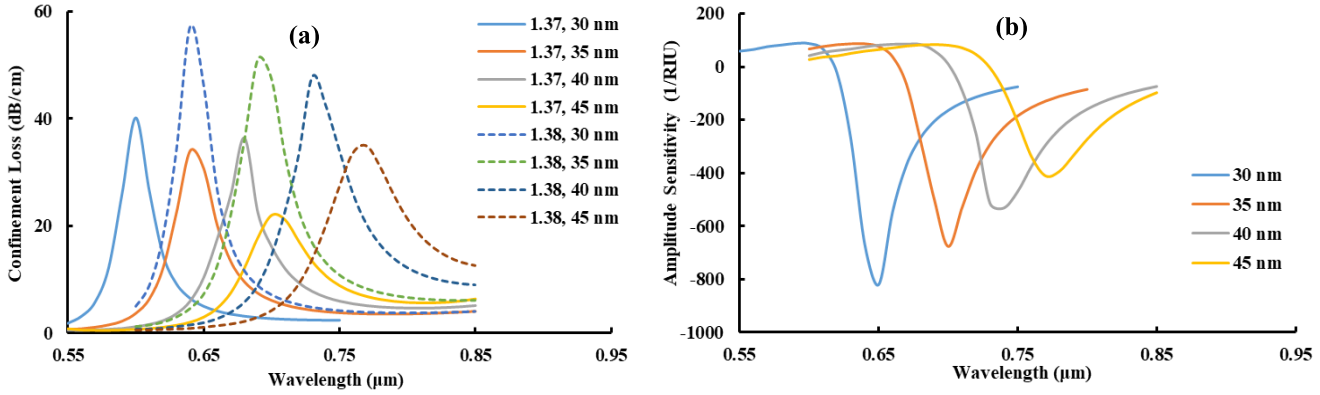

FIGURE 5. Influence of variation of gold layer thickness from 30 nm to 45 nm on (a) The confinement loss, and (b) The AS of the proposed sensor for y-polarization of light.

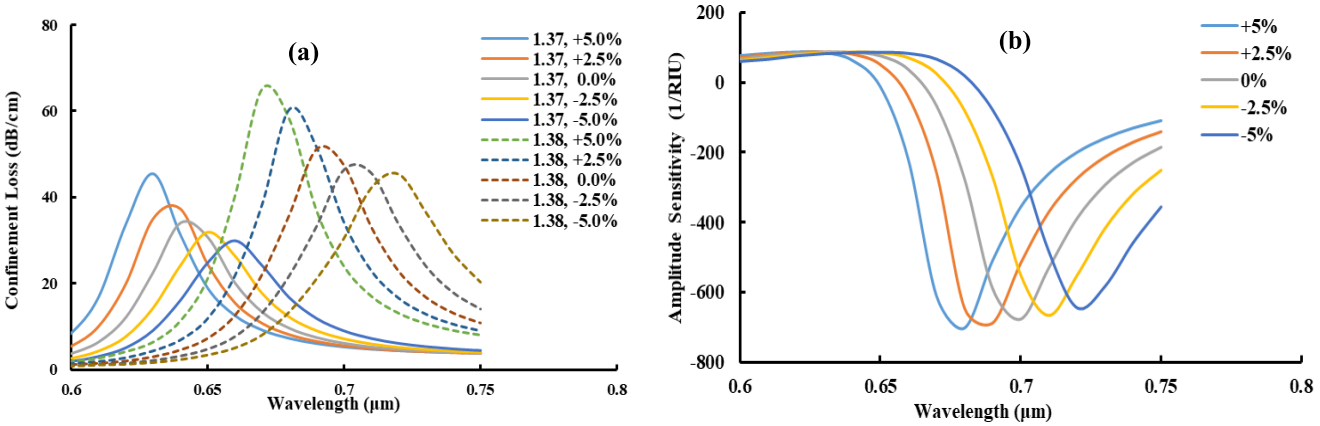

FIGURE 6. Variation of (a) Confinement loss, and (b) Amplitude sensitivity of the proposed sensor for y-polarization of light due to pitch modulation up to ± 5% of the specified value.

phenomenon for lowering the value of pitch. Furthermore, Fig. 6 (b) indicates the effect of variation of pitch on AS of the sensor where the AS curves can be observed moving toward a shorter wavelength with the increase in pitch and vice versa with an approximately equal magnitude. Fig. 7 (a)–(b) demonstrates the effect of altering the air holes diameter on the spectral loss and AS. In Fig. 7(a), the solid and dotted lines represent the confinement loss for analyte RI of 1.37 and 1.38, respectively. It is observed that the confinement loss has been increased and shifted towards a shorter wavelength when the size of the air holes decreases as a broader path is produced to move the light from the center to the surface of the sensor. Also, the AS curve shifts to a shorter wavelength while reducing the air hole size as indicated in Fig. 7(b). On the other hand, the opposite effect is found as the air holes increase in diameter.

V. OPERATION AND PRACTICAL DETECTION SCHEME

The detection process of *Pseudomonas* bacteria is highly dependent on the adsorption of microbes on the sensor surface causing the sensing medium to change in RI. Water with an RI of 1.33 is considered as a sensing medium in this structure. As a matter of fact, the RI of the sensing medium is contingent upon the culture concentration and motility of *Pseudomonas* bacteria which ranges from 1.33 to 1.40 for different culture concentrations and motility [2], [3]. While the underlying principle of the sensor proposed in this study is demonstrated by complete numerical simulation, the functional sensing scheme is demonstrated in Fig. 8. A light source called optical tunable source (OTS) is required in the input side of the scheme which can produce multi-wavelength light. To monitor the light spectra obtained from the sensor, an optical spectrum analyzer (OSA) is attached at the output side of the sensor. The OTS and OSA are connected with the sensor through a polarization-maintaining fiber (PMF) [32], [52]. The analyte which is previously cultured in the laboratory is placed at the outer periphery of the sensor. Inlet and outlet pipes are engaged to control the flow of the sensing medium by using a pump [32]. The effective RI of the sensor alters when the sample to be sensed comes in contact with the sensor, causing the SPR curve to shift to a longer or shorter wavelength as depicted in Fig. 8 by the red or blue dotted curves, respectively. The corresponding shift in SPR angle is monitored via the OSA. Finally, the unknown analytes can be easily identified by examining the shifting in SPR wavelength using the computer [44].

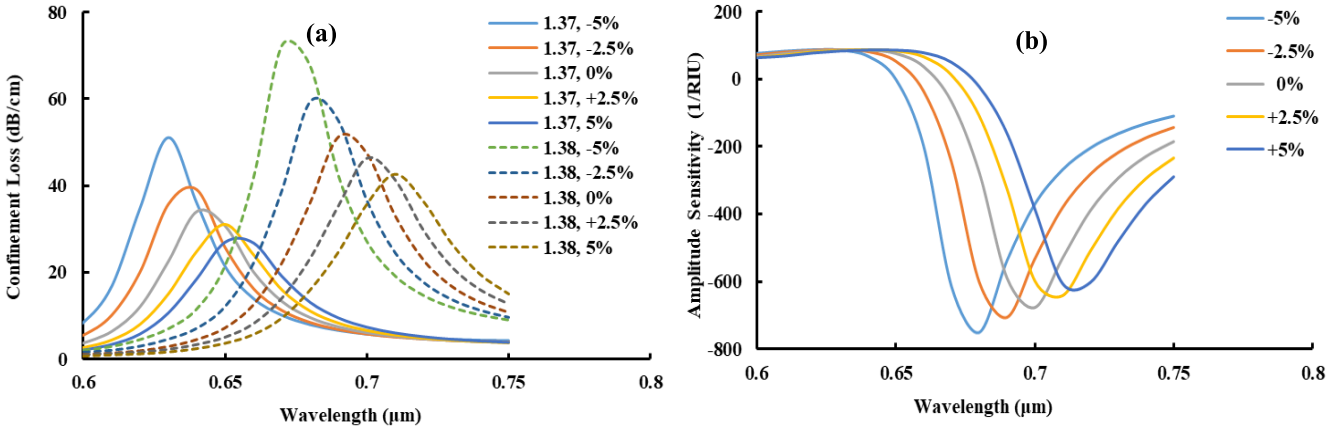

FIGURE 7. Variation of (a) Confinement loss, and (b) Amplitude sensitivity of the proposed sensor for y-polarization of light due to variation in air holes diameter up to ± 5% of the designed value.

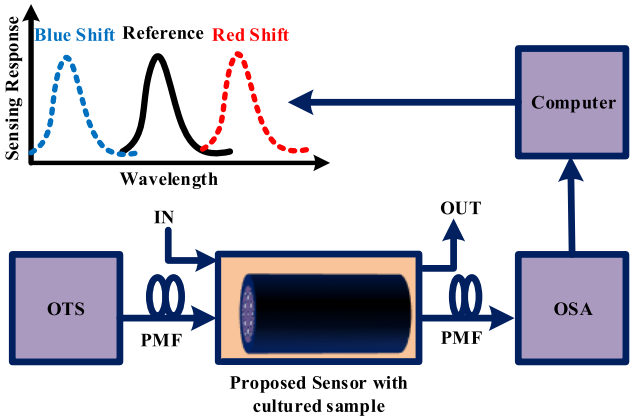

FIGURE 8. Framework for detecting pseudomonas bacteria using the proposed sensor.

VI. CONCLUSION

In this work, a simple round-shaped PCF based SPR sensor operating on WI and AI method rather than angular interrogation for the detection of *Pseudomonas* bacteria is proposed. The confinement loss and the phase matching point are numerically evaluated by utilizing the FEM for sensing medium RI of 1.33 to 1.42. According to numerical results, the proposed sensor reveals quite a high WS and AS of 20,000 nmRIU^{-1} and 1380 RIU^{-1}, respectively. Furthermore, the sensor shows an improved FOM with a value of 470.59 RIU^{-1}. Upon considering the variation of geometrical parameters during fabrication, the sensor performance is carried out by varying the structural parameters up to ± 5% from its designed value. As the proposed sensor has demonstrated promising sensing characteristics with a simple architecture, it can be an exciting platform in the biosensing field, especially for *Pseudomonas* bacteria detection.

ACKNOWLEDGMENT

The authors wish to thank Md. Aslam Mollah, Department of ETE, RUET, Bangladesh for their valuable suggestions.

REFERENCES

[1] Z. Hossain, "Bacteria: Pseudomonas," *Encycl Food Saf*, vol. 1, pp. 490–500, 2014.

[2] N. Mudgal, P. Yupapin, J. Ali, and G. Singh, "$BaTiO_3$-graphene-affinity layer-based surface plasmon resonance (SPR) biosensor for pseudomonas bacterial detection," *Plasmonics*, vol. 15, pp. 1221–1229, Mar. 2020.

[3] A. S. Kushwaha, A. Kumar, R. Kumar, M. Srivastava, and S. K. Srivastava, "Zinc oxide, gold and graphene-based surface plasmon resonance (SPR) biosensor for detection of pseudomonas like bacteria: A comparative study," *Optik*, vol. 172, pp. 697–707, Nov. 2018.

[4] J. Homola and M. Piliarik, "Surface plasmon resonance (SPR) sensors," in *Surface Plasmon Resonance Based Sensors*. Springer, 2006, pp. 45–67.

[5] R. Otupiri, E. K. Akowuah, S. Haxha, H. Ademgil, F. AbdelMalek, and A. Aggoun, "A novel birefrigent photonic crystal fiber surface plasmon resonance biosensor," *IEEE Photon. J.*, vol. 6, no. 4, Aug. 2014, Art. no. 6801711.

[6] J. Ortega-Mendoza, A. Padilla-Vivanco, C. Toxqui-Quitl, P. Zaca-Morán, D. Villegas-Hernández, and F. Chávez, "Optical fiber sensor based on localized surface plasmon resonance using silver nanoparticles photodeposited on the optical fiber end," *Sensors*, vol. 14, no. 10, pp. 18701–18710, Oct. 2014.

[7] E. K. Akowuah, T. Gorman, H. Ademgil, S. Haxha, G. K. Robinson, and J. V. Oliver, "Numerical analysis of a photonic crystal fiber for biosensing applications," *IEEE J. Quantum Electron.*, vol. 48, no. 11, pp. 1403–1410, Nov. 2012.

[8] A. A. Rifat, R. Ahmed, A. K. Yetisen, H. Butt, A. Sabouri, G. A. Mahdiraji, S. H. Yun, and F. M. Adikan, "Photonic crystal fiber based plasmonic sensors," *Sens. Actuators B, Chem.*, vol. 243, pp. 311–325, May 2017.

[9] H. R. Stuart and D. G. Hall, "Enhanced dipole-dipole interaction between elementary radiators near a surface," *Phys. Rev. Lett.*, vol. 80, no. 25, p. 5663, 1998.

[10] A. A. Rifat, G. A. Mahdiraji, Y. G. Shee, M. J. Shawon, and F. R. M. Adikan, "A novel photonic crystal fiber biosensor using surface plasmon resonance," *Procedia Eng.*, vol. 140, pp. 1–7, Jan. 2016.

[11] L. Wu, J. Guo, Q. Wang, S. Lu, X. Dai, Y. Xiang, and D. Fan, "Sensitivity enhancement by using few-layer black phosphorus-graphene/TMDCs heterostructure in surface plasmon resonance biochemical sensor," *Sens. Actuators B, Chem.*, vol. 249, pp. 542–548, Oct. 2017.

[12] Y. Zhao, R.-J. Tong, F. Xia, and Y. Peng, "Current status of optical fiber biosensor based on surface plasmon resonance," *Biosensors Bioelectron.*, vol. 142, Oct. 2019, Art. no. 111505.

[13] M. M. Rahman, M. M. Rana, M. S. Rahman, M. S. Anower, M. A. Mollah, and A. K. Paul, "Sensitivity enhancement of SPR biosensors employing heterostructure of PtSe2 and 2D materials," *Opt. Mater.*, vol. 107, Sep. 2020, Art. no. 110123.

[14] M. S. Rahman, M. S. Anower, and L. F. Abdulrazak, "Modeling of a fiber optic SPR biosensor employing tin selenide (SnSe) allotropes," *Results Phys.*, vol. 15, Dec. 2019, Art. no. 102623.
[15] X. Jiang and Q. Wang, "Refractive index sensitivity enhancement of optical fiber SPR sensor utilizing layer of MWCNT/PtNPs composite," *Opt. Fiber Technol.*, vol. 51, pp. 118–124, Sep. 2019.
[16] H. Fu, M. Zhang, J. Ding, J. Wu, Y. Zhu, H. Li, Q. Wang, and C. Yang, "A high sensitivity D-type surface plasmon resonance optical fiber refractive index sensor with graphene coated silver nano-columns," *Opt. Fiber Technol.*, vol. 48, pp. 34–39, Mar. 2019.
[17] A. B. Siddik, S. Hossain, A. K. Paul, M. Rahman, and A. Mollah, "High sensitivity property of dual-core photonic crystal fiber temperature sensor based on surface plasmon resonance," *Sens. Bio-Sens. Res.*, vol. 29, Aug. 2020, Art. no. 100350.
[18] A. A. Rifat, G. A. Mahdiraji, Y. M. Sua, Y. G. Shee, R. Ahmed, D. M. Chow, and F. R. M. Adikan, "Surface plasmon resonance photonic crystal fiber biosensor: A practical sensing approach," *IEEE Photon. Technol. Lett.*, vol. 27, no. 15, pp. 1628–1631, Aug. 1, 2015.
[19] A. Rifat, G. Mahdiraji, D. Chow, Y. Shee, R. Ahmed, and F. Adikan, "Photonic crystal fiber-based surface plasmon resonance sensor with selective analyte channels and graphene-silver deposited core," *Sensors*, vol. 15, no. 5, pp. 11499–11510, May 2015.
[20] F. Haider, R. A. Aoni, R. Ahmed, M. S. Islam, and A. E. Miroshnichenko, "Propagation controlled photonic crystal fiber-based plasmonic sensor via scaled-down approach," *IEEE Sensors J.*, vol. 19, no. 3, pp. 962–969, Feb. 2019.
[21] Y. Tang, J. Zou, C. Ma, Z. Ali, Z. Li, X. Li, M. Ma, X. Mou, Y. Deng, L. Zhang, and K. Li, "Highly sensitive and rapid detection of Pseudomonas aeruginosa based on magnetic enrichment and magnetic separation," *Theranostics*, vol. 3, no. 2, p. 85, 2013.
[22] N. Tijet, D. Boyd, S. N. Patel, M. R. Mulvey, and R. G. Melano, "Evaluation of the Carba NP test for rapid detection of carbapenemase-producing Enterobacteriaceae and Pseudomonas aeruginosa," *Antimicrobial Agents Chemotherapy*, vol. 57, no. 9, pp. 4578–4580, Sep. 2013.
[23] G. Bodelón, V. Montes-García, V. López-Puente, E. H. Hill, C. Hamon, M. N. Sanz-Ortiz, S. Rodal-Cedeira, C. Costas, S. Celiksoy, I. Pérez-Juste, L. Scarabelli, A. La Porta, J. Pérez-Juste, I. Pastoriza-Santos, and L. M. Liz-Marzán, "Detection and imaging of quorum sensing in Pseudomonas aeruginosa biofilm communities by surface-enhanced resonance Raman scattering," *Nature Mater.*, vol. 15, no. 11, pp. 1203–1211, Nov. 2016.
[24] A. Verma, A. Prakash, and R. Tripathi, "Performance analysis of graphene based surface plasmon resonance biosensors for detection of pseudomonas-like bacteria," *Opt. Quantum Electron.*, vol. 47, no. 5, pp. 1197–1205, May 2015.
[25] A. Verma, A. Prakash, and R. Tripathi, "Sensitivity improvement of graphene based surface plasmon resonance biosensors with chaclogenide prism," *Optik*, vol. 127, no. 4, pp. 1787–1791, Feb. 2016.
[26] B. D. Gupta and R. K. Verma, "Surface plasmon resonance-based fiber optic sensors: Principle, probe designs, and some applications," *J. Sensors*, vol. 2009, Jun. 2009, Art. no. 979761.
[27] W. Qin, S. Li, Y. Yao, X. Xin, and J. Xue, "Analyte-filled core self-calibration microstructured optical fiber based plasmonic sensor for detecting high refractive index aqueous analyte," *Opt. Lasers Eng.*, vol. 58, pp. 1–8, Jul. 2014.
[28] M. R. Hasan, M. I. Hasan, and M. S. Anower, "Tellurite glass defect-core spiral photonic crystal fiber with low loss and large negative flattened dispersion over S+ C+ L+ U wavelength bands," *Appl. Opt.*, vol. 54, no. 32, pp. 9456–9461, 2015.
[29] A. Vial, A. Grimault, D. Macias, D. Barchiesi, and M. de la Chapelle, "Application to the modeling of improved analytical fit of gold dispersion: Extinction spectra with a finite-difference time-domain method," *Phys. Rev. B, Condens. Matter*, vol. 71, Feb. 2005, Art. no. 085416.
[30] R. A. Aoni, R. Ahmed, M. M. Alam, and S. Razzak, "Optimum design of a nearly zero ultra-flattened dispersion with lower confinement loss photonic crystal fibers for communication systems," *Int. J. Sci. Eng. Res*, vol. 4, pp. 1–4, Jan. 2013.
[31] G. Wang, S. Li, G. An, X. Wang, Y. Zhao, W. Zhang, and H. Chen, "Highly sensitive D-shaped photonic crystal fiber biological sensors based on surface plasmon resonance," *Opt. Quantum Electron.*, vol. 48, no. 1, p. 46, Jan. 2016.
[32] M. M. Rahman, M. M. Rana, M. S. Anower, M. S. Rahman, and A. K. Paul, "Design and analysis of photonic crystal fiber-based plasmonic micro-biosensor: An external sensing scheme," *Social Netw. Appl. Sci.*, vol. 2, no. 7, pp. 1–11, Jul. 2020.
[33] Y. Lu, C.-J. Hao, B.-Q. Wu, M. Musideke, L.-C. Duan, W.-Q. Wen, and J.-Q. Yao, "Surface plasmon resonance sensor based on polymer photonic crystal fibers with metal nanolayers," *Sensors*, vol. 13, no. 1, pp. 956–965, Jan. 2013.
[34] M. S. Aruna Gandhi, K. Senthilnathan, P. R. Babu, and Q. Li, "Visible to near infrared highly sensitive microbiosensor based on surface plasmon polariton with external sensing approach," *Results Phys.*, vol. 15, Dec. 2019, Art. no. 102590.
[35] J. T. Robinson, K. Preston, O. Painter, and M. Lipson, "First-principle derivation of gain in high-index-contrast waveguides," *Opt. Exp.*, vol. 16, no. 21, pp. 16659–16669, 2008.
[36] T. D. Visser, H. Blok, B. Demeulenaere, and D. Lenstra, "Confinement factors and gain in optical amplifiers," *IEEE J. Quantum Electron.*, vol. 33, no. 10, pp. 1763–1766, Oct. 1997.
[37] G. A. Mahdiraji, D. M. Chow, S. R. Sandoghchi, F. Amirkhan, E. Dermosesian, K. S. Yeo, Z. Kakaei, M. Ghomeishi, S. Y. Poh, S. Y. Gang, and F. R. M. Adikan, "Challenges and solutions in fabrication of silica-based photonic crystal fibers: An experimental study," *Fiber Integr. Opt.*, vol. 33, nos. 1–2, pp. 85–104, Jan. 2014.
[38] P. J. A. Sazio, "Microstructured optical fibers as high-pressure microfluidic reactors," *Science*, vol. 311, no. 5767, pp. 1583–1586, Mar. 2006.
[39] M. B. E. Griffiths, P. J. Pallister, D. J. Mandia, and S. T. Barry, "Atomic layer deposition of gold metal," *Chem. Mater.*, vol. 28, no. 1, pp. 44–46, Dec. 2015.
[40] M. F. H. Arif and M. J. H. Biddut, "A new structure of photonic crystal fiber with high sensitivity, high nonlinearity, high birefringence and low confinement loss for liquid analyte sensing applications," *Sens. Bio-Sens. Res.*, vol. 12, pp. 8–14, Feb. 2017.
[41] H. Ademgil and S. Haxha, "PCF based sensor with high sensitivity, high birefringence and low confinement losses for liquid analyte sensing applications," *Sensors*, vol. 15, no. 12, pp. 31833–31842, Dec. 2015.
[42] M. J. B. M. Leon and M. A. Kabir, "Design of a liquid sensing photonic crystal fiber with high sensitivity, bireferingence & low confinement loss," *Sens. Bio-Sens. Res.*, vol. 28, Jun. 2020, Art. no. 100335.
[43] M. S. Islam, J. Sultana, A. A. Rifat, R. Ahmed, A. Dinovitser, B. W.-H. Ng, H. Ebendorff-Heidepriem, and D. Abbott, "Dual-polarized highly sensitive plasmonic sensor in the visible to near-IR spectrum," *Opt. Exp.*, vol. 26, no. 23, pp. 30347–30361, 2018.
[44] M. A. Mollah, S. M. R. Islam, M. Yousufali, L. F. Abdulrazak, M. B. Hossain, and I. S. Amiri, "Plasmonic temperature sensor using D-shaped photonic crystal fiber," *Results Phys.*, vol. 16, Mar. 2020, Art. no. 102966.
[45] A. K. Paul, "Design and analysis of photonic crystal fiber plasmonic refractive Index sensor for condition monitoring of transformer oil," *OSA Continuum*, vol. 3, pp. 2253–2263, Aug. 2020.
[46] J. Lou, T. Cheng, S. Li, and X. Zhang, "Surface plasmon resonance photonic crystal fiber biosensor based on gold-graphene layers," *Opt. Fiber Technol.*, vol. 50, pp. 206–211, Jul. 2019.
[47] G. P. Mishra, D. Kumar, V. S. Chaudhary, and G. Murmu, "Cancer cell detection by a heart-shaped dual-core photonic crystal fiber sensor," *Appl. Opt.*, vol. 59, no. 33, pp. 10321–10329, 2020.
[48] X. Sun, N. Li, B. Zhou, W. Zhao, L. Liu, C. Huang, L. Ma, and A. R. Kost, "Non-enzymatic glucose detection based on phenylboronic acid modified optical fibers," *Opt. Commun.*, vol. 416, pp. 32–35, Jun. 2018.
[49] L. Zeni, C. Perri, N. Cennamo, F. Arcadio, G. D'Agostino, M. Salmona, M. Beeg, and M. Gobbi, "A portable optical-fibre-based surface plasmon resonance biosensor for the detection of therapeutic antibodies in human serum," *Sci. Rep.*, vol. 10, no. 1, Dec. 2020, Art. no. 11154.
[50] M. B. Hossain, M. M. Islam, L. F. Abdulrazak, M. M. Rana, T. B. A. Akib, and M. Hassan, "Graphene-coated optical fiber SPR biosensor for $BRCA_1$ and $BRCA_2$ breast cancer biomarker detection: A numerical design-based analysis," *Photon. Sensors*, vol. 10, no. 1, pp. 67–79, Mar. 2020.
[51] R. Funari, K.-Y. Chu, and A. Q. Shen, "Detection of antibodies against SARS-CoV-2 spike protein by gold nanospikes in an opto-microfluidic chip," *Biosensors Bioelectron.*, vol. 169, Dec. 2020, Art. no. 112578.
[52] M. A. Mahfuz, M. A. Hossain, E. Haque, N. H. Hai, Y. Namihira, and F. Ahmed, "A bimetallic-coated, low propagation loss, photonic crystal fiber based plasmonic refractive index sensor," *Sensors*, vol. 19, no. 17, p. 3794, Sep. 2019.

N. JAHAN was born in Jessore, Bangladesh, in 1998. She is currently pursuing the B.Sc. degree in engineering with the Department of Electrical and Computer Engineering (ECE), Rajshahi University of Engineering and Technology (RUET), Rajshahi, Bangladesh. Her research interests include the design of sensors and biosensors for biomedical applications.

MD. M. RAHMAN was born in Narsingdi, Dhaka, Bangladesh, in 1992. He received the B.Sc. degree in electrical and electronic engineering (EEE) from the Rajshahi University of Technology (RUET), Rajshahi, Bangladesh. He is currently a Lecturer with the Department of Electrical and Computer Engineering (ECE), RUET. His research interests include sensors and biosensors technology, photonics and optoelectronic devices, optical fiber communications, and biomedical applications.

MOMINUL AHSAN received the B.Sc. degree from the Department of Computer Science and Engineering, State University of Bangladesh, Dhaka, Bangladesh, in 2008, the M.Eng. degree (Research) from the Faculty of Engineering and Computing, Dublin City University, Dublin, Ireland, in 2014, and the Ph.D. degree from the School of Computing and Mathematical Sciences, University of Greenwich, London, U.K., in 2019. He is a Postdoctoral Researcher with the Department of Engineering, Manchester Metropolitan University. His research interests include prognostics, data analytics, machine learning, reliability, power electronics, wireless communication, and wearable technology. He is currently a Member of the Institution of Engineering and Technology (MIET), U.K., an Associate Fellow of Higher Education Academy (AFHEA), U.K., and an Associate Member of Bangladesh Computer Society. He was a recipient of M.Eng. stipend at Dublin City University in 2010, the Ph.D. scholarship at University of Greenwich in 2014, and the Excellent Poster Award in the IEEE International Spring Seminar on Electronic Technology, Sofia, Bulgaria in 2017.

MD. ABDUL BASED (Member, IEEE) was born in Nilphamari, Bangladesh, in 1979. He received the B.S. degree in computer science and engineering from Dhaka International University, Dhaka, Bangladesh, in 2000, the M.S. degree in computer science from North South University, in 2005, and the M.S. degree in information and communication systems security (ICSS) from the Royal Institute of Technology (KTH), in 2008. From 2008 to 2014, he worked as a Research Fellow with the Norwegian University of Science and Technology (NTNU), Trondheim, Norway, on the security aspects of electronic voting. Since 2014, he has been an Associate Professor with the Electrical, Electronics and Telecommunication Engineering (EETE) Department, and the Head of Computer Science and Engineering Department, at Dhaka International University, Dhaka. Since 1st September, he has been working as the Head of the Department Of Electrical, Electronics, and Telecommunication Engineering (EETE), Dhaka International University. Besides teaching and research, he also worked as IT and MIS Specialist in a Government Project at Ministry of Planning, Dhaka, Bangladesh. He is an expert of Curriculum Design and Development, and Outcome Based Education. His research interests include information security, electronic voting, and cryptographic protocols. Associate Professor Based is a life-time member as well as elected councilor of Bangladesh Computer Society (BCS), Bangladesh.

MD. MASUD RANA received the Ph.D. degree in electrical engineering from the University of Technology Sydney (UTS), Sydney, Australia, in 2013. He joined as a Lecturer with the Department of Electrical and Electronic Engineering, RUET, Bangladesh, in 2006, where he is currently a Professor. He has authored and coauthored over 70 journal and conference papers. His research interests include modeling of the biosensor, computational methods for microwave device modeling, EM propagation modeling, and antenna modeling and designing. He hold awards and honors, include the IPRS and UTS President Scholarship at UTS; the ICEEE 2015 Best Paper Award; the University Gold Medal in 2007, RUET; the EEE Association Award in 2003 and 2005, RUET.

SARAVANAKUMAR GURUSAMY (Member, IEEE) was born in Seithur, Tamil Nadu, India. He received the B.Eng. degree in electronics and instrumentation engineering from the National Engineering College, Kovilpatti, India, in 2004, the master's degree in control and instrumentation engineering from the Thiagarajar College of Engineering, Madurai, in 2007, and the Ph.D. degree from the Faculty of Instrumentation and Control Engineering, Kalasalingam Academy of Research and Education (KARE), India, in 2017. In 2009, he joined the Department of Instrumentation and Control Engineering, KARE, as a Lecturer. In 2011, he was an Assistant Professor. He served as a Lecturer with the Department of Electrical and Computer Engineering, University of Gondar, Ethiopia, from 2014 to 2018. Then, he joined back to KARE as a Senior Assistant Professor, where he served for a year. He is currently serving as an Associate Professor with the Department of Electrical and Electronics Technology, Federal TVET Institute, Addis Ababa, Ethiopia. His current research interests include virtual instrumentation, applications of evolutionary algorithms for control problem, nonlinear system identification, multivariable PID controller, model predictive control, autonomous vehicle, and mobile robotics.

JULFIKAR HAIDER is currently working as a Senior Lecturer in mechanical engineering with the Department of Engineering, Manchester Metropolitan University, U.K. He has been supervising research associates and Ph.D. Students in the above areas. He has received funding by Innovate U.K. to conduct Eight Knowledge Transfer Partnership projects with industry worth more than a million pound. He has published and presented over 80 technical papers in international journals, conferences and books. His main research interests include materials processing, thin film coating, composite materials, finite element analysis, and artificial intelligence; and it is in these areas that he is renowned for his work both Nationally and Internationally, which is justified by his research outputs in International journals and conferences. He is serving as the Executive Editor for the International Journal published by Taylor and Francis *Advances in Materials and Processing Technologies*.